Determination of Combustion Kinetic Parameters and Fuel Properties of Hydrochar Prepared from Hydrothermal Carbonization of Bamboo

Pei-Yong Ma,[a] Su-Wei Shi,[a] Fang-Yu Fan,[b,c] Yu-Qing Wang,[a,*] Xian-Wen Zhang,[b] and Xian-Jun Xing [b]

The hydrothermal treatment of bamboo was carried out to investigate the effects of different temperatures (230 °C, 260 °C) and residence times (30 min, 60 min) on the combustion behaviors and properties of hydrochar. The higher heating value (HHV) increased gradually with increasing hydrothermal temperature and residence time, while the energy yield decreased. It was found that 260 °C and 30 min with a HHV of 22.8 MJ/kg and an energy yield of 57.8% were appropriate parameters for the production of hydrochar. The atomic oxygen/carbon ratio indicated that the upgrading process converted the bamboo into fuel that was similar to clean solid fuel with a high energy density. The thermal gravimetric analysis showed that the temperature and the residence time had noticeable impacts on the combustion behavior and the activation energy of hydrochar. The combustion reaction ability and rate were greatly improved when the hydrochar was prepared at temperatures greater than 200 °C. The activated energy value was determined by the model-free methods, of which Kissinger-Akahira- Sunose (KAS), Flynn-Wall-Ozawa (FWO) were the most appropriate for this purpose and resulted in similar values.

Keywords: Combustion kinetics; Fuel properties; Hydrothermal carbonization; Bamboo

*Contact information: a: School of Mechanical Engineering, Hefei University of Technology, Hefei, Anhui 230009, PR China; b: Advanced Energy Technology and Equipment Research Institute, Hefei University of Technology, Hefei, Anhui 230009, PR China; c: The College of Forestry, Southwest Forestry University, Kunming, Yunnan 650224, PR China; *Corresponding author: yuqingw@mail.ustc.edu.cn*

INTRODUCTION

China is rich in agricultural and forestry resources, and biomass energy has broad prospects for economic development. The efficiency of thermal combustion of biomass raw materials is not high because of their natural drawbacks, including high moisture content and low energy density (Wei *et al.* 2015). Bamboo is a type of biomass material that has been widely cultivated in the west and south of China. Bamboo is a great potential bio-energy resource for the future because of its abundance and fast growth capacity. The total area covered by bamboo in China is more than five million hectares (Tan *et al.* 2011). To date, little information is available about bamboo being used as biomass fuel. Liu *et al.* (2013a) studied the effect of moisture content on bamboo pellets and investigated the effect of carbonization conditions (temperature and time) on the properties of bamboo pellets. In the preliminary research, the direct utilization of bamboo was limited because of the high contents of moisture and volatile matter, which made the combustion process more difficult to control.

Hydrothermal carbonization (HTC) can be used to treat biomass that contains high contents of moisture without drying (He *et al.* 2013). Hydrochar is a kind of charcoal that is formed through hydrothermal carbonization of biomass. Compared with the raw biomass, the hydrochar has better fuel properties, such as higher carbon content, lower oxygen content, higher hydrophobicity, higher heating value, higher energy density, and lower emission of greenhouse gases (Kang *et al.* 2012). Therefore, hydrochar application to renewable energy has been put forward as a tool to relieve the energy crisis and mitigate global warming in recent years.

Currently, a lot of information can be obtained about hydrothermal carbonization of biomass for the preparation of hydrochar to be applied as a biofuel (Ben and Ragauskas 2012; Reza *et al.* 2014a). For instance, Liu *et al.* (2013b) pretreated waste biomass by the hydrothermal carbonization process to improve the fuel properties. They demonstrated that the higher heating value (HHV) of hydrochar increased with increasing hydrothermal carbonization temperature, whereas the mass yield decreased. Funke and Ziegler (2010) defined HTC as the combined dehydration and decarboxylation of a fuel to raise its carbon content, with the aim of achieving a higher calorific value. However, most researchers characterize the standard fuel properties of hydrochar, such as element content, HHV, and mass and energy yields. In addition, only a few studies have paid attention to the combustion behavior and kinetic parameters of hydrochar.

Therefore, the objective of this preliminary work was to determine moderate conditions for hydrochar preparation of bamboo with improved fuel properties and combustion performances. The work focused on three research areas in order to investigate the effects of the HTC temperature and residence time: hydrochar characteristics, thermal combustion behavior, and calculations of the combustion kinetics. Results from this research can be helpful to provide theoretical guidance on the application of hydrochar combustion.

EXPERIMENTAL

Material

Bamboo was obtained from Guangde County, Xuancheng City, which is located in the southeastern part of Anhui Province (China). The raw material was dried at 105 °C for 12 h, crushed using a commercial laboratory blender (Benchen Electromechanical Equipment Corp., Hebei, China), and then ground and sieved into fines (180 to 200 mesh).

Hydrochar Preparation

Two series of experiments were addressed to study the effects of temperature and residence time on the products. In the two series, bamboo powders were thermally treated at various temperatures (200, 230, or 260 °C with a 10 °C /min heating rate), with residence times of 30 or 60 min. In a typical experiment, 2.4 g of dry bamboo powder combined with 40 mL of deionized water was weighed and transferred into a micro high-pressure reactor (Kemi Technology Corp., Anhui, China). The working volume of the reactor was 50 mL. The mixture was stirred using a magnetic mixer for 15 min at 300 rpm, and then the reactor was tightly closed. N_2 was charged into the reactor to dispel the air. The pressure was not controlled and was kept autogenic with the water. At the end of the residence period, the heater was turned off and the reactor was immersed into cold water as soon as possible to stop the reaction. The mixture was filtered and cleaned by anhydrous alcohol and deionized

water 3 to 5 times. Then, the hydrochar was dried at 105 °C until its weight reached a constant value for the subsequent combustion. Hydrochar samples are designated XXX-YY, where XXX indicates the temperature and YY is the residence time. For example, 200-30 represents hydrochar prepared at 200 °C for 30 min.

Combustion

Combustion experiments were performed using a thermo-gravimetric (TG-DTG) device (SETSYS Evo, Setaram Corp., France). Experiments were carried out with the bamboo powder and corresponding hydrochar samples (~10 mg) with a constant flow of simulated air (60 mL/min). The simulated air was composed of N_2 and O_2 in a ratio of 4:1. All experiments were conducted in the temperature range of 20 to 900 °C with three different heating rates (10, 20, or 40 K/min).

Elemental Analysis of Bamboo and Hydrochar

Elemental contents of samples were determined using an elemental analyzer (Vario Micro cube, Elementar, Germany). The oxygen content was obtained by subtraction. The values were represented as the mean ± standard deviation (n=3).

Analysis of Mass Yield, Energy Yield, and Higher Heating Value (HHV)

The mass yields R_0 and the energy yields R_1 were calculated using Eqs. 1 and 2, respectively. HHVs were calculated from their elemental contents using Eq. 3 (Sheng and Azevedo 2005), where C, H, and N denote the carbon, hydrogen, and nitrogen contents of bamboo or hydrochar on a dry mass percentage, respectively. The equations are as follows:

$$R_0 = \frac{m_{char}}{m_0} \times 100\% \quad (1)$$

where m_{char} denotes the mass of hydrochar and m_0 is the mass of raw bamboo;

$$R_1 = \frac{HHV_{char}}{HHV_0} \times R_0 \times 100\% \quad (2)$$

where HHV_{char} denotes the higher heating value of hydrochar and HHV_0 is that of raw bamboo; and

$$HHV = -1.3675 + 0.3137 \times [C] + 0.7009 \times [H] + 0.0318 \times [O] \quad (3)$$

where [*C*] refers to the mass fraction of carbon, [*H*] is that of hydrogen, and [*O*] indicates that of oxygen.

Kinetic Models

In this paper, three kinds of model-free models, including the KAS, FWO, and FR methods, were used to calculate kinetic parameters. Model-free models do not involve the assumption of the function mechanism. At least three thermal analysis curves were needed to reduce the influence of different heating rates variances. At the same conversion rate, the value of f(*a*) and G(*a*) does not vary with the heating rate, which can lead to more reliable activation energy *E* without introducing a dynamic model (Anca-Couce *et al.* 2014; Ceylan and Topçu 2014).

The kinetic equation of the isothermal homogeneous residence system was used in the non-isothermal heterogeneous system. Moreover, the dynamic equation of the non-isothermal heterogeneous residence is as follows,

$$\frac{d\alpha}{dT}=\frac{A}{\beta}\exp(-\frac{E}{RT})f(\alpha) \quad (4)$$

where α refers to the conversion ratio, T is temperature, A is a pre-exponential factor, β is the heating rate, E is the activation energy, R is the gas constant (8.314L/mol · K), and $f(\alpha)$ denotes the kinetics mechanism function.

FWO model

The FWO (Garcia-Maraver *et al.* 2015) model uses Doyle's approximation. The activation energy and the frequency factor are obtained at every conversion from a plot of the common logarithm of heating rate log(β) against 1/T, which represents a linear relationship with a given value of conversion at different heating rates (Eq. 5),

$$\log(\beta)=\log(\frac{AE}{RG(\alpha)})-2.315-0.4567\frac{E}{RT_\alpha} \quad (5)$$

where $G(\alpha)$ denotes the most probable mechanism function. Here, $G(\alpha)$ is constant at a given value of conversion. Additionally, a first-order residence (n = 1) is considered, which is expressed by Eq. 6:

$$G(\alpha)=n^{-1}(-1+(1-\alpha)^{-n}) \quad (6)$$

KAS model

The KAS model is based on Eq. 7. Kinetics parameters can be obtained from a plot of $\ln(\frac{\beta}{T^2})$ *versus* $\frac{1}{T_\alpha}$ for a given value of conversion from 0.2 to 0.8. As mentioned before in the FWO method, $G(\alpha)$ is constant at a given value of conversion, and a first order reaction(n =1) was considered.

$$\ln(\frac{\beta}{T^2})=\ln(\frac{AE}{RG(\alpha)})-\frac{E}{RT_\alpha} \quad (7)$$

FR model

The FR model is a differential non-isothermal approach commonly used to determine the kinetic triplet parameters by employing Eq. 8. The model is based on the inter-comparison $\ln(\frac{d\alpha}{dt})$ for a given fraction of conversion *versus* the reciprocal of temperature at linear heating rates. The activation energy and frequency factor can be calculated at each given fraction of conversion α. The apparent activation energy is determined from the slope of (-E/R), and the frequency factor is obtained from the intercept ln A(1-α) at the first order:

$$\ln(\frac{\mathrm{d}\alpha}{\mathrm{d}t}) = \ln(A) + n\ln(1-\alpha) - \frac{E}{RT} \quad (8)$$

RESULTS AND DISCUSSION

Combustion Behaviors of Bamboo and Hydrochar

Figure 1 shows TG and DTG profiles of the raw bamboo and corresponding derived hydrochars. For a better evaluation of different combustion behaviors, the entire combustion profile was divided into several stages, depending on the rate of weight loss in the DTG curve. According to Yang *et al.* (2004), three main stages are observed during the thermal decomposition of samples at three heating rates. These stages consisted of water evaporation (T < 200 °C), oxidative degradation of the biomass (200 < T < 600 °C), and oxidation of the charred residue (T > 600 °C). As for heating rates, DTG showed a similar shape. From 230 to 400 °C, the TGA profile showed the highest weight loss, which indicated the decomposition of hemicellulose and cellulose. When the temperature was between 400 °C and the burnout temperature, the DTG curve showed smaller and broad-shaped peaks, indicative of lignin decomposition. Additionally, the mass loss was less dramatic. As shown in Fig. 1, both the first peak and the second one in the DTG curves of all samples shifted to higher temperatures, which indicated that weight losses occurred at increasing temperatures when the heating rates increased from 10 to 40 K/min. Because a stronger thermal shock was acquired in a short time and a greater temperature gradient between the inside and outside the sample developed (Wang *et al.* 2012), there was a greater limitation of heat transfer.

TG and DTG comparison curves of samples at 20 K/min can be seen in Fig. 2, where the combustion behaviors of bamboo noticeable changed after hydrothermal carbonization. Considering the hydrochar prepared for 30 min at different temperatures as examples, both of the peaks in the DTG curves shifted toward the right after the hydrothermal carbonization. Compared with the raw bamboo, the weight loss rate at the first peak of both hydrochar prepared at 200 °C, 30 min (HC200-30) and HC230-30 increased, while that of HC260-30 decreased. Sharp DTG peaks of HC200-30 and HC230-30 implied that there was incomplete combustion, with low efficiency and high pollutant emission (carbon monoxide and polycyclic aromatic hydrocarbon) (Khan *et al.* 2009). The weight loss rate at the second peak for all samples, except HC260-30, were lower than that corresponding to the first peak. The first weight loss peak of HC260-30 and HC260-60 gradually disappeared, which indicated that the volatile matter had disappeared. It is interesting to note that the first peak of HC260-30 displays a lower weight loss rate compared with that of the second peak, which is different from results reported by Yang *et al.* (2016). In Yang's study, the hydrothermal carbonization time was 10 min at 260 °C. This may mean the longer hydrothermal carbonization time (more than 10 min) at 260 °C can lead to a greater release of volatile matter, which indicates that a greater portion of the aromatic structure in the lignin is destroyed during the hydrothermal carbonization. Combustion behaviors of the hydrochar prepared for 60 min at different temperatures were almost similar to that of the hydrochar prepared for 30 min. Nevertheless, as shown in Fig. 1, the first peak of HC260-60 was not as obvious as that of HC260-30, which indicated that a longer residence time at 260 °C can promote the release of volatile matter.

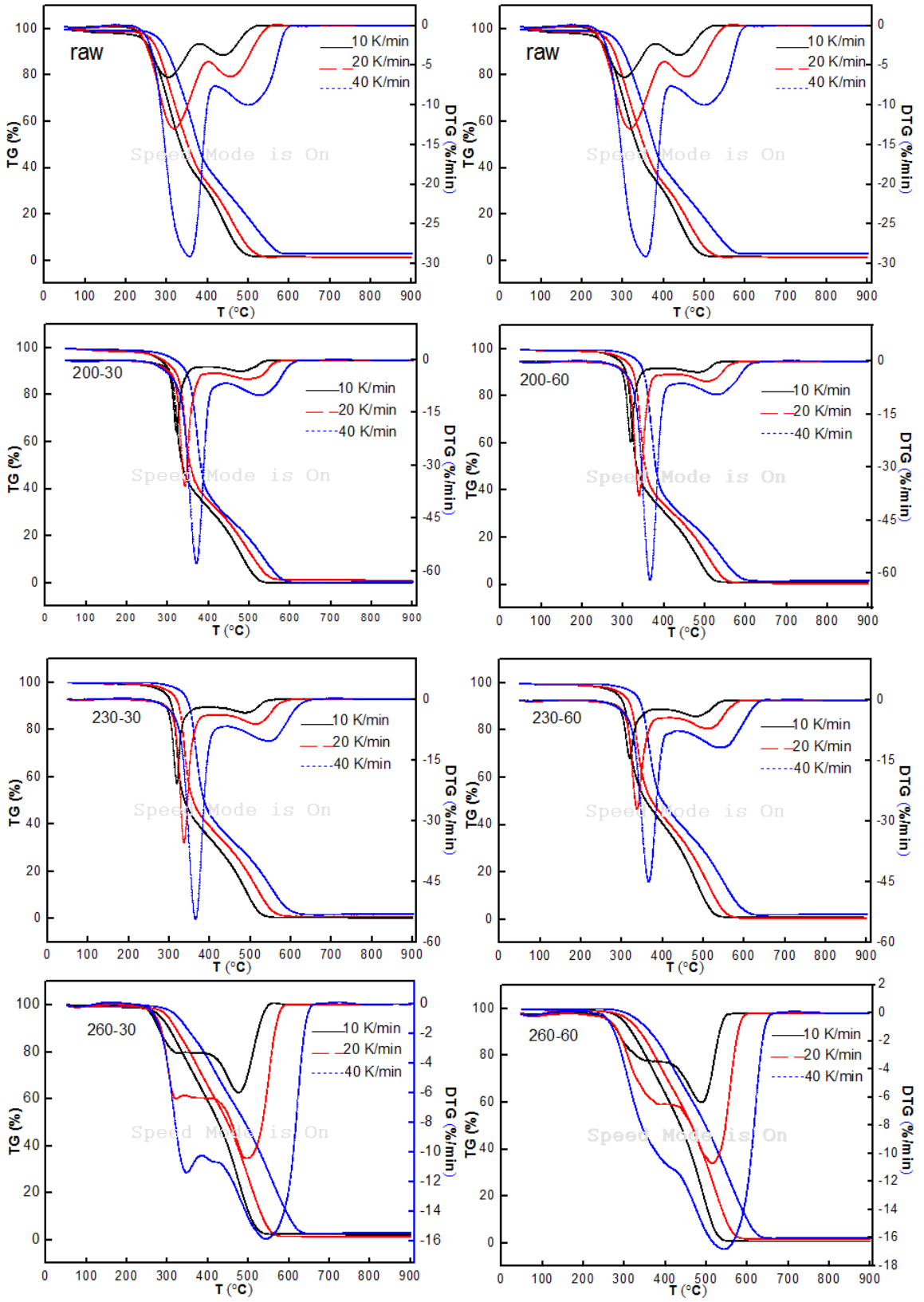

Fig. 1. TG and DTG curves of bamboo and hydrochars at different heating rates

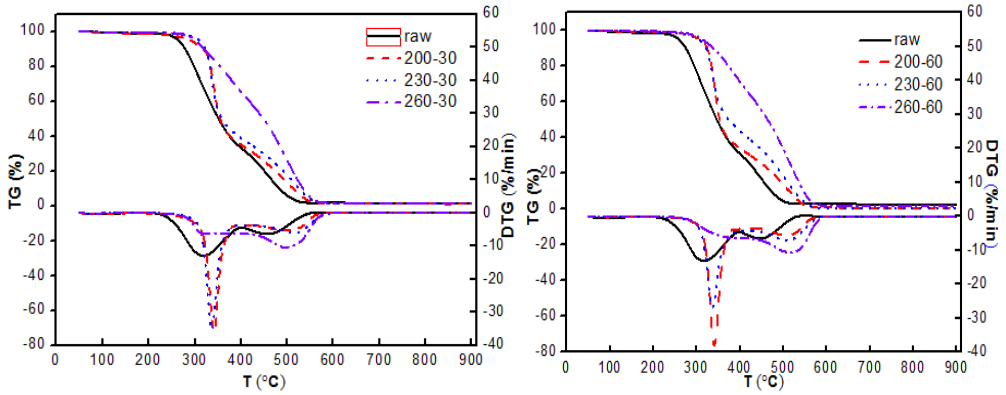

Fig. 2. TG and DTG comparison curves of samples heated at 20 K/min

Fuel Properties and Combustion Characteristic Parameters of Bamboo and Hydrochar

Fuel properties of bamboo and hydrochar

Table 1 shows the fuel properties of raw bamboo and hydrochar. Elemental analysis revealed an increase in carbon percentage and a proportional decrease in hydrogen and oxygen contents, which caused higher value of HHV (Nizamuddin *et al*. 2015b). Compared with raw bamboo, the carbon content of hydrochar increased with increasing hydrothermal treatment temperature, while the hydrogen and oxygen contents decreased. The calorific value of hydrochar increased with higher temperatures. The calorific value of hydrochar increased when the HTC has been performed at high temperatures.

The van-Krevelen diagram can be used as a useful way to describe the fuel characteristics of a solid fuel through the elemental concentration (Reza *et al.* 2014b). In a typical van-Krevelen diagram, the ratio of atomic hydrogen and carbon is plotted against the ratio of the atomic oxygen and carbon. Such a van-Krevelen diagram is presented in Fig. 3 for the different hydrochars produced in this study. A better solid fuel can be found close to the origin of the van-Krevelen diagram, and *vice versa* (Reza *et al.* 2014c). Not surprisingly, the raw bamboo was located in the upper right corner of the Van-Krevelen diagram, and the hydrochars tended to be located closer the origin. In fact, with higher HTC temperatures, the hydrochar moved closer to the origin. As shown in Fig. 3, hydrochars prepared at 260 °C were closest to the origin, followed by hydrochars prepared at 230 °C. The temperature had a more noticeable influence on the fuel characteristics than the residence time. Generally, a solid fuel farther away from the origin means more energy loss, and more water vapor and smoke generation during combustion (Liu *et al*. 2013). Furthermore, Fig. 3 shows that H/C and O/C had a linear relationship (R^2 = 0.999) with respect to both HTC temperature and residence time, which indicates that the main dehydration occurred in the HTC process. The higher temperature led to an extensive dehydration and an increase in the degree of the condensation of hydrochar (Jain *et al.* 2015). Therefore, these results suggest that the combustion behavior was improved after undergone a hydrothermal carbonization process.

As shown in Table 1, the mass yield was negatively correlated with the HHV. With increasing temperature, the mass yield of hydrochar decreased and the HHV increased. Thus, the energy yield is introduced as a comprehensive evaluation index to evaluate the fuel characteristics of hydrochar.

Table 1. Fuel Properties of Samples Obtained at Different Temperatures

Sample	*C*(%)	*H*(%)	*O*(%)	N(%)	S(%)	*O* /C	*H*/C	*HHV* (MJ/kg)	R_0(%)	R_1(%)
raw	45.92 ±0.12	5.97 ±0.09	47.31 ±0.11	0.48 ±0.01	0.32 ±0.02	0.77 ±0.10	1.56 ±0.11	18.73 ±0.10	—	—
200-30	49.78 ±0.15	5.95 ±0.03	43.69 ±0.09	0.36 ±0.02	0.22 ±0.03	0.66 ±0.12	1.43 ±0.09	19.81 ±0.12	58.75 ±0.21	62.14 ±0.16
230-30	55.03 ±0.23	5.93 ±0.13	38.63 ±0.15	0.20 ±0.02	0.21 ±0.01	0.53 ±0.18	1.29 ±0.20	21.28 ±0.20	52.55 ±0.32	59.70 ±0.25
260-30	60.53 ±0.09	5.92 ±0.16	33.12 ±0.15	0.23 ±0.01	0.20 ±0.02	0.41 ±0.12	1.17 ±0.12	22.82 ±0.14	47.48 ±0.30	57.85 ±0.28.
200-60	54.42 ±0.11	5.93 ±0.21	39.21 ±0.19	0.21 ±0.03	0.23 ±0.01	0.54 ±0.16	1.31 ±0.18	21.11 ±0.20	55.95 ±0.38	63.06 ±0.31
230-60	58.02 ±0.24	5.90 ±0.25	35.59 ±0.24	0.25 ±0.02	0.24 ±0.00	0.46 ±0.24	1.22 ±0.24	22.10 ±0.24	47.75 ±0.48	56.34 ±0.35
260-60	63.01 ±0.29	5.90 ±0.17	30.68 ±0.19	0.20 ±0.01	0.21 ±0.02	0.37 ±0.22	1.12 ±0.25	23.51 ±0.23	40.13 ±0.36	50.37 ±0.32

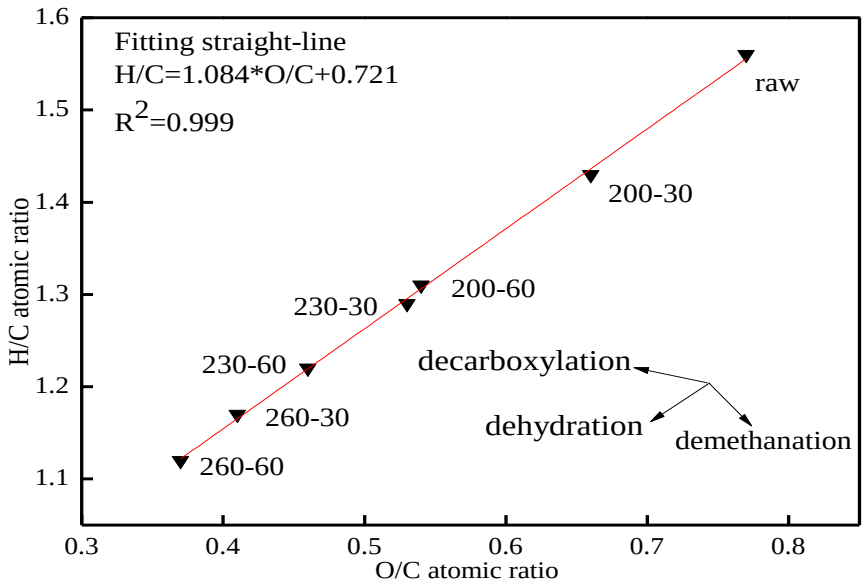

Fig. 3. van-Krevelen diagram of raw bamboo and hydrochar

Figure 4 shows the HHV and energy yield of hydrochar obtained in this study. The HHV of hydrochar increased with increasing hydrothermal temperature or time, while the energy yield decreased. Generally, the fuel properties of bamboo were elevated after the hydrothermal carbonization. Hydrochar prepared at 260 °C for 60 min possessed the highest HHV (23.51 MJ/kg), a 25.5% increase compared with that of raw bamboo. This increase in HHV is attributable to the respective destruction and generation of low-energy chemical bonds and high-energy chemical bonds, respectively (Boussarsar *et al.* 2009). However, the energy yield of the HC260-60 was the lowest (50.4%), which is not favorable for industrial applications. When one considers both HHV and energy yield, the hydrochar prepared at 260 °C for 30 min possessed better fuel properties, such as high HHV (22.82 MJ/kg), an increase of 21.9% compared to that of raw bamboo, and a higher energy yield (57.8%) than that of HC260-60. This HHV is comparable to that of loblolly pine dry

torrefied at 250 °C for 80 min (20.9 MJ/kg), an increase of 6.6% compared with that of raw loblolly pine (Yan *et al.* 2009), which indicates that hydrothermal carbonization is much more effective at increasing the HHV of biomass than dry torrefaction. Kambo and Dutta (2014) also reported that HTC pellets showed considerably superior physicochemical properties when compared with raw and torrefied pellets. To conclude, it was determined that the fuel properties of bamboo can be upgraded by hydrothermal carbonization, and the hydrochar prepared at 260 °C for 30 min possesses the most appropriate fuel properties, with rather high HHV and energy yield.

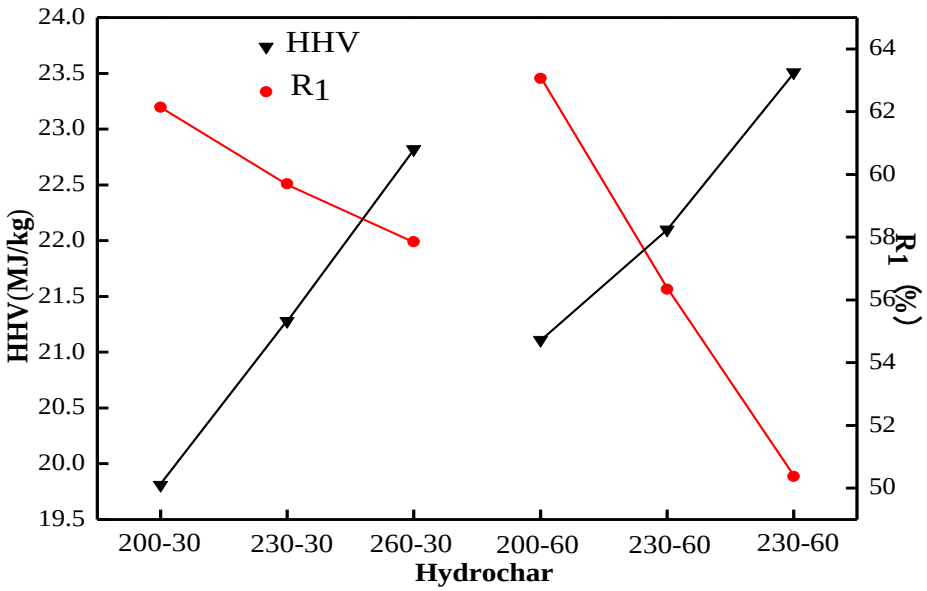

Fig. 4. HHV and energy yield curves of hydrochar

Combustion parameters of bamboo and hydrochar

The comprehensive combustibility index (*S*) was used to evaluate the combustion reactivity of samples,

$$S_N = \frac{(dw/dt)_{max}(dw/dt)_{mean}}{T_i^2 T_h}, \quad (9)$$

where $(dw/dt)_{max}$ and $(dw/dt)_{mean}$ represent the maximum and mean rates of weight loss (wt.%/min), respectively. Moreover, T_i and T_h denote the ignition and burnout temperature, respectively.

The combustion parameters of raw bamboo and hydrochars at three different heating rates are given in Table 2. With an increase in the heating rate, the comprehensive combustibility index S_N increased and the combustion performance is improved, which shows that a higher heating rate is beneficial to the improvement of the combustion performance.

The S_N value of hydrochars at a heating rate of 20 K/min was considered in more detail. As presented in Table 2, S_N represents the combustion reactivity of the hydrochars. The S_N increased when the hydrothermal temperature was decreased. Moreover, the S_N of hydrochars, except the hydrochar prepared at 260 °C, were higher than that of the raw bamboo. This result can be ascribed to the higher $(dw/dt)_{max}$ of hydrochar prepared at 200

or 230 °C, which leads to the destruction of long-chain polymers (*e.g.*, cellulose and hemicellulose) and the formation of short-chain hydrocarbons after hydrothermal carbonization (Boussarsar *et al*. 2009). The burnout temperature of hydrochars was higher than that of raw bamboo with an increase in temperature. Thus, both the hydrothermal temperature and the residence time can affect combustion parameters because of changes in the hydrochar decomposition during the HTC process. The temperature factor is more considerable than the effect of the residence time. Similar results have been reported by other researchers (Nizamuddin *et al*. 2015b).

Table 2. Combustion Parameters of Samples

Sample	B (K·min $^{-1}$)	T_i (K)	T_h (K)	$(dw/dt)_{max}$ (%·min^{-1})	$(dw/dt)_{mean}$ (%·min^{-1})	S_N (10^{-7})
raw	10	543.45	759.26	6.50	3.88	1.12
raw	20	552.2	788.46	12.97	7.26	4.21
raw	40	566.6	835.6	29.10	13.79	14.95
200-30	10	581.83	790.95	20.36	4.10	3.13
200-30	20	598.29	818.35	35.67	7.75	9.44
200-30	40	621.21	846.24	57.68	15.34	27.18
230-30	10	579.9	800.08	20.83	3.97	3.07
230-30	20	596.2	829.23	35.40	7.55	9.07
230-30	40	620.05	866.65	54.37	14.17	23.12
260-30	10	550.54	797.01	5.96	3.74	0.92
260-30	20	561.14	829.68	10.40	7.12	2.84
260-30	40	576.87	891.17	15.84	12.28	6.56
200-60	10	580.92	787.40	22.77	4.20	3.60
200-60	20	600.89	819.93	37.98	7.88	10.11
200-60	40	622.43	841.04	61.93	15.50	29.46
230-60	10	578.94	796.52	14.29	4.02	2.15
230-60	20	591.89	828.83	26.84	7.61	7.04
230-60	40	617.76	870.29	44.74	13.97	18.81
260-60	10	565.71	802.72	6.35	3.94	0.97
260-60	20	580.43	840.01	10.68	7.22	2.72
260-60	40	607.55	893.01	16.80	12.91	6.58

Combustion reaction kinetics parameters for bamboo and hydrochar

Figure 5 shows results obtained by isoconversional kinetic models. It can be observed that activation energy (E) is highly dependent on the conversion, which means that the combustion of hydrochars and raw bamboo involves a complex process with different reactions (Ceylan and Topçu 2014) at the same combustion stage. The analysis of results indicates that the values of E calculated from the KAS and FWO models are similar for each combustion stage, and their variations with conversion are almost coincident. E calculated from the FR model displays the same regularity with the conversion rate. From the calculation of HC230-30 using the FR model, it can be observed that the activation energy reaches the maximum value at 0.5, then it decreases at 0.6, with a slight increase at 0.7. According to other studies (Lu *et al.* 2009), the FR model varies irregularly when the conversation rate exceeds 50%. Because of the abnormal results calculated using the FR model, the following analyses are based on results from the FWO and KAS models. The maximum activation energy of each sample is in the fixed carbon combustion stage, which

shows that the energy consumption of the initial stage of the fixed carbon combustion is the highest. Taking the result calculated from the FWO model as an example, *E* intervals for the raw material and samples HC200-30, HC230-30, HC260-30, HC200-60, HC230-60, and HC260-60 were 89 to 126, 89 to 216, 86 to 118, 80 to 90, 89 to 162, 90 to 138, and 91 to 101 kJ/mol, respectively. The activation energy of hydrochar obtained at 260 °C exhibited an indistinctly changing trend and the value scope was smaller than the other ones. Figure 5 shows that the changing trend of the activation energy of samples was not obvious in the conversion range of 0.2 to 0.4 in the volatile combustion stage.

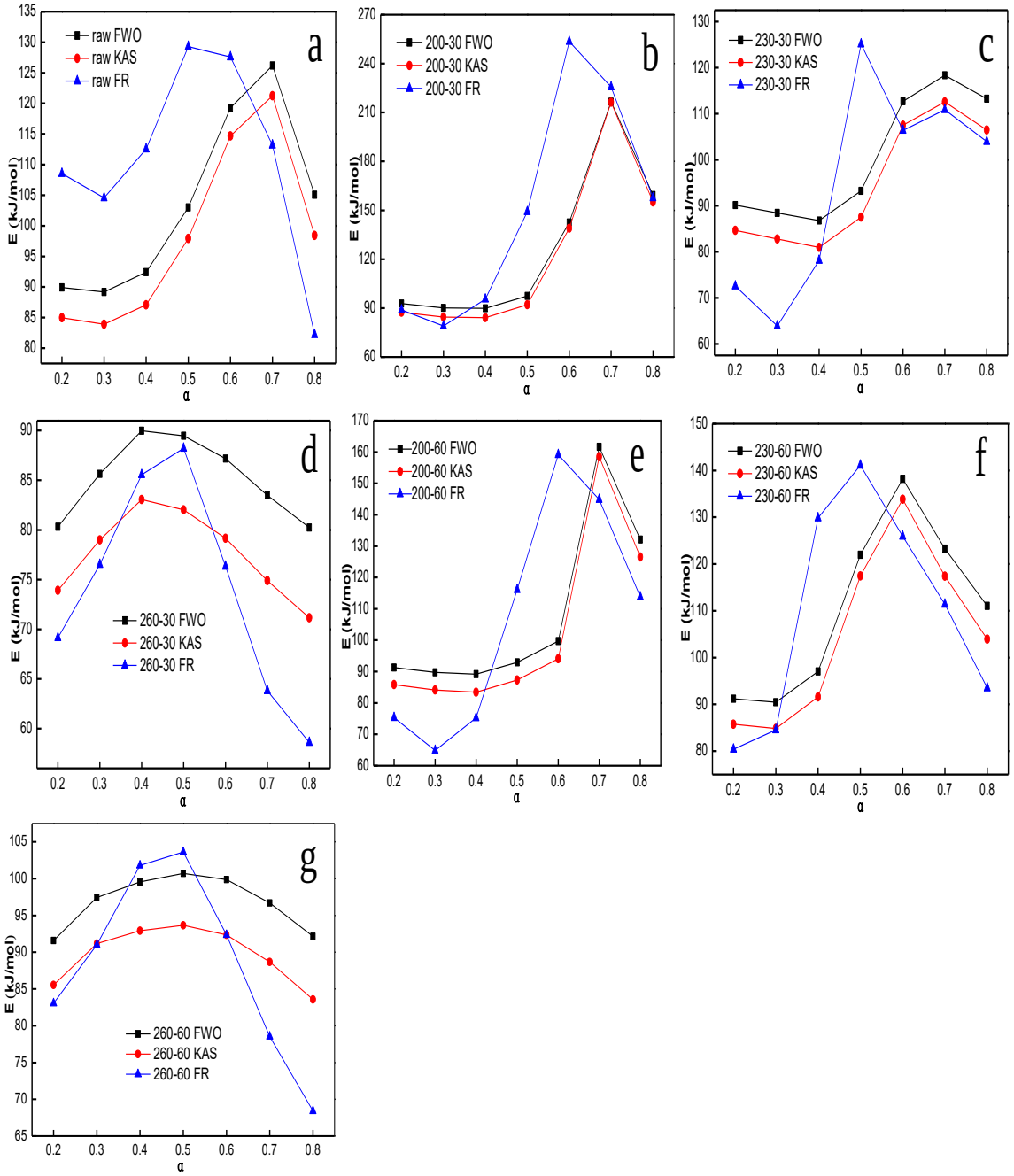

Fig. 5. Changes in activation energy with the progressive conversion of samples for FWO, KAS, and FR models

Figure 6 shows the change in average activation energy and average correlation coefficient at different conversion rates with different samples for FWO, KAS, and FR models. Values of the activation energy and the correlation coefficient in the conversion rate range of 0.2 to 0.8 were averaged. The average correlation coefficients calculated from the FWO and KAS models were all above 0.95, which indicates that the calculation of the activation energy is reliable. It can be found that the abnormal correlation coefficient was 0.91 from the calculation of FR, which illustrates that the FR method can be improved. The activation energy *E* indicates the minimum energy required to cause chemical reactions. In addition, as the activation energy decreases, so does the reaction ability. It can be seen from Fig. 6 that the hydrochar prepared at 260 °C possessed a rather low average activation energy, which can be attributed to the lower contents of volatile matter, as mentioned above. For a residence time of 30 min, the average activation energy values of these hydrochars increased first and then decreased with increasing hydrothermal temperature. Considering results from the FWO model as an example, the average activation energy of the raw material and samples HC200-30, HC230-30, HC260-30, HC200-60, HC230-60, and HC260-60 were 104, 127, 100, 85, 108, 110, and 97 kJ/mol, respectively. Moreover, the reaction abilities of HC230-30, HC260-30, and HC260-60 were also enhanced. However, the reaction ability of sample HC200-30 was less than that of the raw material. Furthermore, the combustion reaction ability and rate were evaluated when the hydrochar was obtained at temperatures greater than 200 °C. Compared with other conditions studied here, the hydrothermal temperature of 260 °C was the most appropriate for the preparation of hydrochar as fuel.

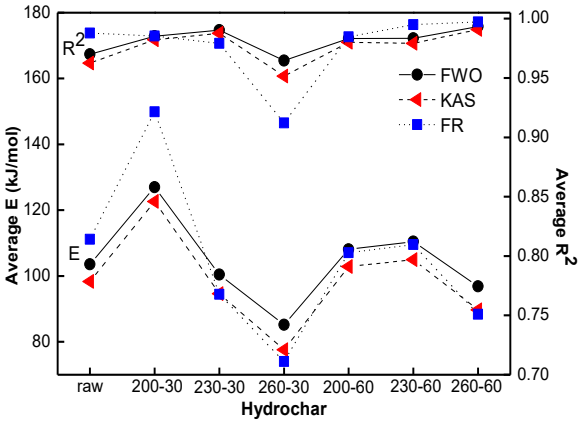

Fig. 6. Changes in the average activation energy and average correlation coefficient at different conversion rates with different samples for FWO, KAS, and FR models

CONCLUSIONS

1. This work provided a detailed observation of the hydrothermal carbonization (HTC) of local bamboo. HTC had a noticeable effect on the combustion behavior and kinetic parameters of bamboo, and the fuel properties of hydrochars were markedly improved.
2. HHV increased gradually with increasing temperature and residence time, while the energy yield decreased. The HTC temperature of 260 °C and residence time of 30 min

was the most suitable reaction condition for hydrochar production. The temperature was more considerable than time in the HTC process.

3. H/C and O/C atomic ratios decreased gradually with increasing hydrothermal temperature and reaction time. The properties of samples HC230-30, HC230-60, HC260-30, and HC260-60 were close to those of lignite. The hydrochar prepared at 260 °C for 30 min possessed better fuel properties, with higher HHV (22.82 MJ/kg) and energy yield (57.85%).
4. The combustion reaction ability and rate were evaluated when the hydrochar was prepared at temperatures greater than 200 °C. The hydrothermal temperature of 260 °C is the most appropriate condition for the preparation of hydrochar as fuel.

ACKNOWLEDGMENTS

The authors are grateful for the support of the Special Fund for Basic Scientific Research Business expenses in the Central University, Grant No. 2013bhzx0034, the China Postdoctoral Science Foundation, Grant No. 2016M590041, the Fundamental Research Funds for the Central Universities, Grant No. JZ2015HGBZ0465 and the Enterprise Research Project, Grant No. W2016JSKF0252.

REFERENCES CITED

Anca-Couce, A., Berger, A., and Zobel N. (2014). "How to determine consistent biomass pyrolysis kinetics in a parallel reaction scheme," *Fuel* 123(1), 230-240. DOI: org/10.1016/j.fuel.2014.01.014

Boussarsar, H., Rogé, B., and Mathlouthi, M. (2009). "Optimization of sugarcane bagasse conversion by hydrothermal treatment for the recovery of xylose," *Bioresource Technology* 100(24), 6537-6542. DOI: 10.1016/j.biortech.2009.07.019

Ben, H., and Ragauskas, A. J. (2012). "Torrefaction of loblolly pine," *Green Chemistry* 14(14), 72-76. DOI: 10.1039/C1GC15570A

Ceylan, S., and Topçu, Y. (2014). "Pyrolysis kinetics of hazelnut husk using thermogravimetric analysis," *Bioresource Technology* 156(4), 182-188. DOI: 10.1016/j.biortech.2014.01.040

Funke, A., and Ziegler, F. (2010). "Hydrothermal carbonization of biomass: A summary and discussion of chemical mechanisms for process engineering," *Biofuels Bioproducts and Biorefining* 4(2), 160-177. DOI: 10.1002/bbb.198

Garcia-Maraver, A., Perez-Jimenez, J. A., Serrano-Bernardo, F., and Zamorano, M. (2015). "Determination and comparison of combustion kinetics parameters of agricultural biomass from olive trees," *Renewable Energy* 83, 897-904. DOI: 10.1016/j.renene.2015.05.049

He, C., Giannis, A., and Wang, J. Y. (2013). "Conversion of sewage sludge to clean solid fuel using hydrothermal carbonization: Hydrochar fuel characteristics and combustion behavior," *Applied Energy* 111(11), 257-266. DOI: 10.1016/j.apenergy.2013.04.084

Jain, A., Balasubramanian, R., and Srinivasan, M. P. (2015). "Hydrothermal conversion of biomass waste to activated carbon with high porosity: A review," *Chemical Engineering Journal* 283, 789-805. DOI: 10.1016/j.cej.2015.08.014

Kang, S. M., Li, X. L., Fan, J., and Chang, J. (2012). "Characterization of hydrochars produced by hydrothermal carbonization of lignin, cellulose, d-xylose, and wood meal," *Industrial and Engineering Chemistry Research* 51(26), 9023-9031. DOI: 10.1021/ie300565d

Kambo, H. S., and Dutta, A. (2014). "Strength, storage, and combustion characteristics of densified lignocellulosic biomass produced via torrefaction and hydrothermal carbonization," *Applied Energy* 135, 182-191. DOI: 10.1016/j.apenergy.2014.08.094

Khan, A. A., Jong, W. De., Jansens, P. J., and Spliethoff, H. (2009). "Biomass combustion in fluidized bed boilers: Potential problems and remedies," *Fuel Processing Technology* 90(1), 21-50. DOI: 10.1016/j.fuproc.2008.07.012

Liu, Z. J., Jiang, Z. H., Cai, Z. Y., Fei, B. H., Yu, Y., and Liu, X. (2013a). "Effects of carbonization conditions on properties of bamboo pellets," *Renewable Energy* 51(2), 1-6. DOI: 10.1016/j.renene.2012.07.034

Liu, Z., Quek, A., Hoekman, S. K., and Balasubramanian, R. (2013b). "Production of solid biochar fuel from waste biomass by hydrothermal carbonization," *Fuel* 103(1), 943-949. DOI: 10.1016/j.fuel.2012.07.069

Lu, C., Song, W., and Lin, W. (2009). "Kinetics of biomass catalytic pyrolysis," *Biotechnology Advances* 27(5), 583-587. DOI: 10.1016/j.biotechadv.2009.04.014

Nizamuddin, S., Jayakumar, N. S., Sahu, J. N., Ganesan, P., Bhutto, A. W., and Mubarak, N. M. (2015a). "Hydrothermal carbonization of oil palm shell," *Korean Journal of Chemical Engineering* 32(9), 1-9. DOI: 10.1007/s11814-014-0376-9

Nizamuddin, S., Mubarak, N. M., Tiripathi, M., Jayakumar, N. S., Sahu, J. N., and Ganesan, P. (2015b). "Chemical, dielectric and structural characterization of optimized hydrochar produced from hydrothermal carbonization of palm shell," *Fuel*, 163, 88-97. DOI: 10.1016/j.fuel.2015.08.057

Reza, M. T., Uddin, M. H., Lynam, J. G., Hoekman, S. K., and Coronella, C. J. (2014a). "Hydrothermal carbonization of loblolly pine: Reaction chemistry and water balance," *Biomass Conversion and Biorefinery* 4(4), 311-321. DOI: 10.1007/s13399-014-01159

Reza, M. T., Andert, J., Wirth, B., Busch, D., Pielert, J., Lynam, J. G., and Mumme J. (2014b). "Hydrothermal carbonization of biomass for energy and crop production," *Applied Bioenergy* 1(1), 11-29. DOI: 10.2478/apbi-2014-0001

Reza, M. T., Wirth, B., Lüder, U., and Werner, M. (2014c). "Behavior of selected hydrolyzed and dehydrated products during hydrothermal carbonization of biomass," *Bioresource Technology* 169(5), 352-361. DOI: 10.1016/j.biortech.2014.07.010

Sheng, C., and Azevedo, J. L. T. (2005). "Estimating the higher heating value of biomass fuels from basic analysis data," *Biomass and Bioenergy* 28(5), 499-507. DOI: 10.1016/j.biombioe.2004.11.008

Tan, Z. Q., Qiu, J. R., Zeng, H. C., Liu, H., and Xiang, J. (2011). "Removal of elemental mercury by bamboo charcoal impregnated with H_2O_2," *Fuel* 90(4), 1471-1475. DOI: 10.1016/j.fuel.2010.12.004

Wang, L., Hustad, J. E., Skreiberg, O., Skjevrak, G., and Grønli, M. (2012). "A critical review on additives to reduce ash related operation problems in biomass combustion applications," *Energy Procedia* 20(5), 20-29. DOI: 10.1016/j.egypro.2012.03.004

Yan, W., Acharjee, T. C., Coronella, C. J., and Vásquez, V. R. (2009). "Thermal pretreatment of lignocellulosic biomass," *Environmental Progress and Sustainable Energy* 28(3), 435-440. DOI: 10.1002/ep.10385

Yang, Y. B., Sharifi, V. N., and Swithenbank, J. (2004). "Effect of air flow rate and fuel moisture on the burning behaviours of biomass and simulated municipal solid wastes in packed beds," *Fuel* 83(11), 1553-1562. DOI: 10.1016/j.fuel.2004.01.016

Yang, W., Wang, H., Zhang, M., Zhu, J., Zhou, J., and Wu, S. (2016). "Fuel properties and combustion kinetics of hydrochar prepared by hydrothermal carbonization of bamboo," *Bioresource Technology* 205, 199-204. DOI: 10.1016/j.biortech.2016.01.068

Article submitted: October 9, 2016; Peer review completed: December 29, 2016; Revised version received and accepted: March 17, 2017; Published: March 23, 2017.
DOI: 10.15376/biores.12.2.3463-3477